

Bacterial Suspensions Deposited on Microbiological Filter Material for Rapid Laser-Induced Breakdown Spectroscopy Identification

Dylan J. Malenfant, Derek J. Gillies, and Steven J. Rehse

Applied Spectroscopy
2016, Vol. 70(3) 485–493
© The Author(s) 2016
Reprints and permissions:
sagepub.co.uk/journalsPermissions.nav
DOI: 10.1177/0003702815626673
asp.sagepub.com



Abstract

Four species of bacteria, *E. coli*, *S. epidermidis*, *M. smegmatis*, and *P. aeruginosa*, were harvested from agar nutrient medium growth plates and suspended in water to create liquid specimens for the testing of a new mounting protocol. Aliquots of 30 μL were deposited on standard nitrocellulose filter paper with a mean 0.45 μm pore size to create highly flat and uniform bacterial pads. The introduction of a laser-based lens-to-sample distance measuring device and a pair of matched off-axis parabolic reflectors for light collection improved both spectral reproducibility and the signal-to-noise ratio of optical emission spectra acquired from the bacterial pads by laser-induced breakdown spectroscopy. A discriminant function analysis and a partial least squares-discriminant analysis both showed improved sensitivity and specificity compared to previous mounting techniques. The behavior of the spectra as a function of suspension concentration and filter coverage was investigated, as was the effect on chemometric cell classification of sterilization via autoclaving.

Keywords

Laser-induced breakdown spectroscopy (LIBS), Pathogen identification, Bacterial classification, Discriminant function analysis (DFA), Partial least squares-discriminant analysis (PLS-DA)

Date received: 27 May 2015; accepted: 17 July 2015

Introduction

The first publications reporting the efficacy of laser-induced breakdown spectroscopy (LIBS) for bacterial identification appeared approximately 12 years ago.^{1–3} Since these initial investigations, considerable effort has been invested in increasing the number and variety of bacterial species and strains that can be identified,^{4–7} investigating the effect that the bacterial mounting surface or growth medium has on the LIBS bacterial spectrum,^{8–11} and enhancing the medical/clinical/professional relevancy of the LIBS-based pathogen diagnostic.^{12–15} The potential to provide information about the metabolic state of the microbiological organism (e.g., reproducing in the log-phase, lysed by autoclave or sonication, dormant due to deposition on an abiotic surface, growing in a biofilm, undergoing bacteriophage induction, or inactivated by bactericidal ultraviolet light exposure) has also been an area of very recent interest.^{8,16,17}

It has been shown in the laboratory that the LIBS technology can provide a rapid, accurate diagnostic for assessing the presence and the species of bacteria in a variety

of samples. This could be extremely useful for medical diagnoses, defense against bioterrorism, and assessments of ecological wellbeing and safety. However, current methods of sample preparation (bacterial mounting protocols) have, for the most part, not been realistic to a clinical setting, typically involving time-consuming steps such as freeze-drying and pelletizing, requiring the use of a bulky centrifuge and other laboratory equipment not common in clinical environments, or mounting on unrealistic platforms that would not typically be used in a clinical pathology laboratory.

In an effort to simplify the preparation protocol, bacterial suspensions have been mounted on disposable nitrocellulose filter paper in place of the commonly used bacto-agar,^{12,18} silicon chips,¹⁴ or glass slides.¹⁹ This has both decreased the time of the preparation process and provided more control

Department of Physics, University of Windsor, Windsor, Ontario, Canada

Corresponding author:

Steven J. Rehse, Department of Physics, University of Windsor, Windsor, Ontario, Canada.
Email: rehse@uwindsor.ca

over the ablation surface while also introducing techniques more reminiscent of those used in a clinical setting

This method of mounting was used to produce a library of 1513 spectra acquired from four bacterial species increasing the statistical significance of the resulting chemometric classification. This is a far greater library size than most other LIBS-based bacterial studies which typically utilize less than 100 spectra per classification category/class. As the intensity of the carbon background in the LIBS spectrum was dependent on the bacterial coverage deposited on the filter, studies were performed to determine the effect of the bacterial suspension concentration on the LIBS spectrum and an attempt was made to determine the concentration required to produce a useful bacterial signal. Lastly, the testing of samples that had been autoclaved (sterilized) prior to testing was also performed.

Apparatus

The apparatus used to perform these LIBS experiments has been described in detail elsewhere,¹¹ although it should be mentioned that, in the interim, this entire apparatus was deconstructed, crated, shipped to a new country, and reassembled in a new facility with slight modifications as described below. A 1064 nm Nd:YAG laser (Spectra Physics LAB-150-10) with 10 ns pulses operating at 10 Hz was used in all experiments. The pulses were focused by a high-damage threshold AR-coated $5\times$ infinite conjugate microscope objective with a long working-distance (LMH-5X-1064, OFR). A CCD camera was placed in line with this objective to allow for observation of the sample as data were collected, as was an alignment He-Ne laser to visualize the laser beam focus on the sample (Figure 1).

Samples were held in the microscope objective focus on a weakly magnetized sample holder inside a newly

constructed Plexiglas argon purge chamber mounted on a manual translation stage. A typical kitchen magnet has field strengths of less than 50 G, which is far too weak to have any effect on LIBS plasma emission.²⁰ This stage could be moved in three dimensions, allowing for focusing on targets of variable height. During data acquisition, the chamber was flushed with argon at a flow rate of 20 SCFH.

Optical emission from the plasma was collected and relayed to the spectrometer via two matched off-axis replicated aluminum parabolic mirrors (3.81 cm diameter, 5.08 cm effective focal length) which focused the light into a 1 m steel-encased multimode optical fiber (core diameter, 600 μm ; numerical aperture [NA], 0.22). The fiber was then coupled to an Echelle spectrometer with a 1024×1024 pixel ($24 \mu\text{m}^2$) intensified charge coupled device (ICCD) camera (LLA Instruments, Inc., ESA3000). The spectrometer provided full spectral coverage in the range of 200–840 nm. The spectrometer was controlled by a personal computer running manufacturer-provided software (ESAWIN v3.20), which controlled both the ICCD shuttering as well as the operation of the laser via an on-board fast-pulse generator. This minimized timing jitter between the laser firing and plasma observation.

The introduction of the parabolic mirrors into the experimental setup increased light collection from the plasma, increasing the apparatus' sensitivity, but also introduced a greater dependency on the location of the target relative to the laser focus in the observed emission. To reproducibly relocate specimens at the appropriate LTSD (lens-to-sample distance) a height alignment system was introduced. A heavily attenuated secondary helium-neon laser (Uniphase Model 155A) illuminated the flat sample through the purge chamber wall at an angle of approximately 45° . Vertical translation of the sample stage resulted in horizontal motion of the laser spot across the sample surface when viewed from above by the CCD camera. An ideal LTSD was determined based on both emission intensity and data reproducibility, and the corresponding position of the attenuated laser spot on the monitor was marked, allowing for realignment of the sample as necessary. To monitor the reproducibility of this LTSD calibration and detect any other day-to-day variations, five single-shot LIBS spectra (preceded by two cleaning pulses) were acquired from five fresh locations on a polished flat steel standard after aligning at the appropriate LTSD. These five spectra were then averaged to create a standard spectrum prior to each day's measurements. In this fashion, the functioning of the system over the course of the entire experiment was quantified.

Previously, the bacterial spectra were approximately background-free due to the use of a watery agar mounting matrix. Use of the 13 mm diameter $0.45 \mu\text{m}$ pore size disposable nitrocellulose filters (EMD Millipore) introduced a significant carbon background signal to the LIBS bacterial spectrum. The intensity of the carbon emission line at

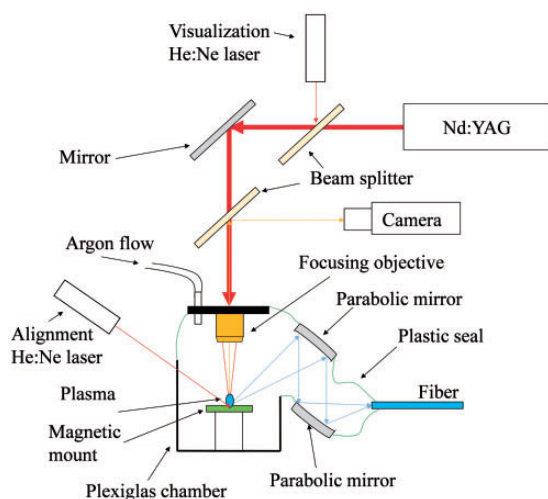


Figure 1. The experimental apparatus utilized in this work.

247 nm limited the image-intensifier amplification that could be used when acquiring weak signals from a small number of cells. While the bacterial signal diminished into the noise as the bacterial cell number was decreased, the strength of the persistent carbon signal from the filter precluded the use of greater amplification which would damage the ICCD at the location of the dispersed 247 nm emission peak.

This study was performed on four bacterial species, *E. coli*, *S. epidermidis*, *M. smegmatis*, and *P. aeruginosa*. These species were chosen for their varying response to the Gram staining procedure, a standard phenotypic classification test. *E. coli* and *P. aeruginosa* are gram negative, *S. epidermidis* is gram positive, and *M. smegmatis* is categorized as an acid-fast bacterium. Bacterial samples were grown at 37 °C on tryptic soy agar (TSA) plates. The time allowed for growth was dependent on species, with *E. coli* and *S. epidermidis* being allowed to grow for 24 h, and *M. smegmatis* and *P. aeruginosa* being grown for 48 h to achieve the same amount of coverage on the TSA plates. Colonies from the plates were transferred to 1.5 mL of distilled water and briefly vortex mixed to create a uniform suspension of cells. Concentration of this suspension was found to be 10^{11} cells/mL via optical densitometry. Bacteria were then transferred to a nitrocellulose filter using a steel disc with three 4.7 mm diameter wells (Figure 2). A total of 30 μ L placed in each well produced three highly-uniform bacterial depositions on the filter with a coverage of approximately 10^9 cells/cm² once dried. Drying was accomplished in a biosafety hood for approximately 25 min. The filter was then mounted on a small piece of flat steel using double-sided tape and the steel was then placed on the translation stage in the sampling purge chamber.

Figure 3 shows LIBS spectra from the blank filter (Figure 3a) and a bacterial deposition on a filter (Figure 3b). LIBS spectra were acquired with a delay of 2 μ s after plasma formation and observed with an ICCD gate width of 20 μ s. These times were chosen as they gave the strongest emission from the observed lines while minimizing the broadband emission characteristic of newly formed plasmas. Spectra were acquired from single shots and the sample stage was translated 0.635 mm between shots. Three single-shot spectra were acquired and digitally averaged to minimize noise, creating a spectral fingerprint comprising three laser shots. Each laser pulse resulted in the ablation of approximately 10^6 cells based on calculations of known cellular concentration and filter coverage. In previous studies, accumulations of five spectra were taken at each location on an agar plate prior to translation and five of these accumulated spectra were then averaged, creating a spectral fingerprint comprising 25 laser shots.¹⁷

Ablation craters in the deposited bacterial pad were measured using scanning electron microscopy and found to be approximately 100 μ m in diameter on average. Microscopy was accomplished using a low-vacuum

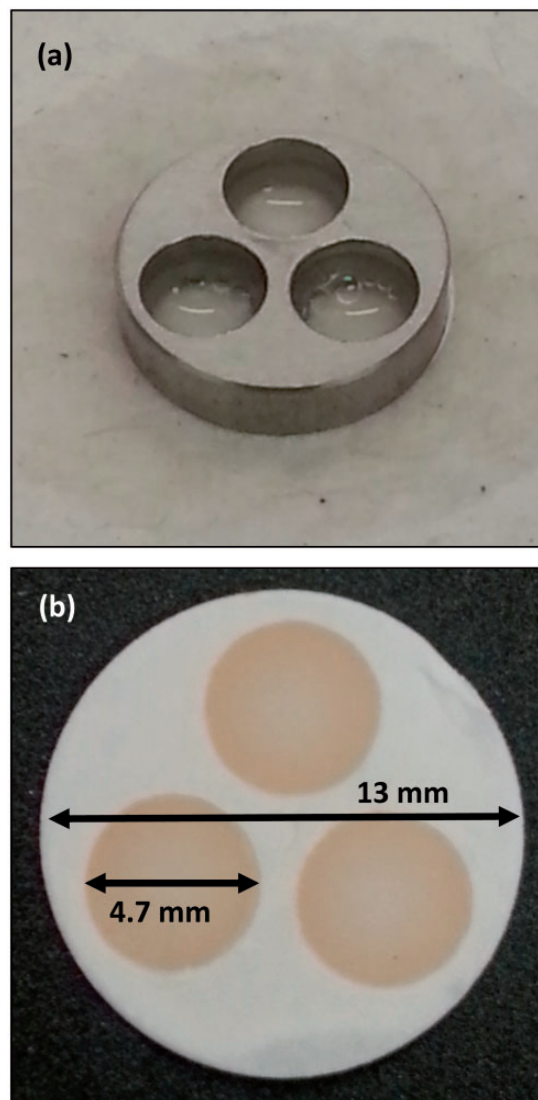


Figure 2. Bacterial mounting for the experiments described in this work. (a) The steel disc with three wells used to create three uniform bacterial depositions on the filter paper. Each well contained 30 μ L of bacterial suspension that was allowed to settle through the filter paper. (b) A dried filter paper after deposition showing the three bacterial pads. About 15–20 spectra of three averaged laser shots were acquired from each circular deposition region.

environmental SEM (Quanta 200 FEG, FEI) without carbon or gold coating. Figure 4a is an SEM image of a freshly deposited *E. coli* pad, Figure 4b is a magnification of that same SEM image with bacterial cells clearly visible, and Figure 4c is an SEM image of a second bacterial pad after laser ablation and data collection. The bacterial pads consistently evidenced smooth, uniform deposition at all magnification scales. Upon drying, the bacterial pad became a hard, glass-like thin film. Cracks which formed when the filter was left to dry could be observed through this film as seen in Figure 4a. These cracks and other

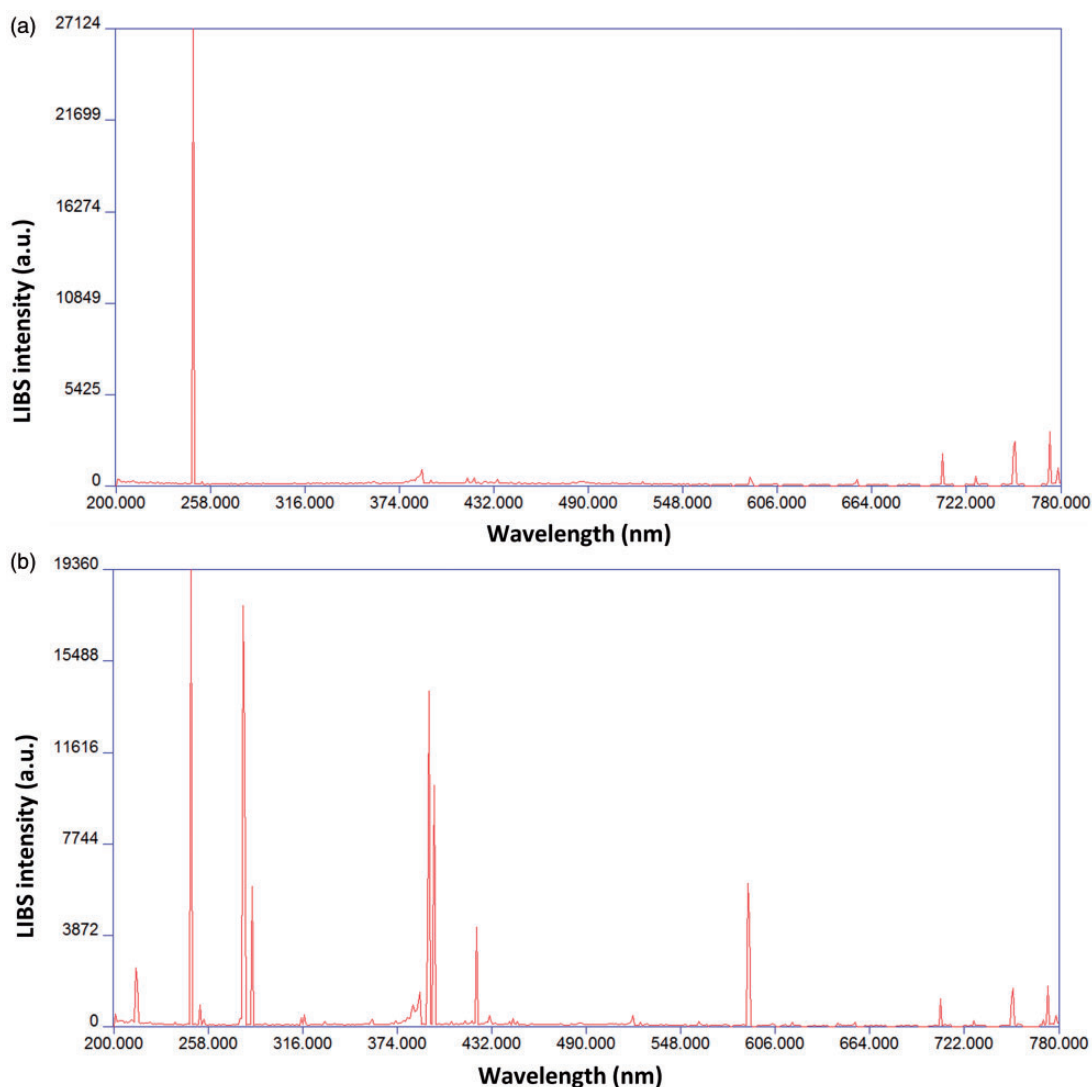


Figure 3. Typical LIBS spectra from (a) a blank nitrocellulose filter and (b) a live bacterial suspension deposited on a filter. Both spectra were acquired in argon 2 μ s after plasma formation and observed with an ICCD gate width of 20 μ s.

evidence of fracturing and uneven ablation were also observed around ablation craters as shown in Figure 4c. These craters showed little sign of melting or thermal damage as might be expected for a bacterial specimen. It is likely that this non-uniform removal of material from the bacterial pad thin-film was the cause of the significantly higher scatter or shot-to-shot variation that was observed in this data compared to the previous ablation on the agar substrate.

Due to an increase in overall signal-to-noise, a new bacterial spectrum discrimination model was created. Our previous model, "ratio-model two" or "RM2," consisted of 80 independent variables, the first 13 of which were merely the intensities of the 13 strongest emission lines observed in the spectrum and the remaining 67 variables were simple ratios of those 13 intensities. The new model which was

referred to as RM3 consisted of 164 independent variables of which 19 were the intensities of the strongest observed atomic emission lines and the remainder were again simple ratios of those intensities. A thorough investigation of the effects of various ratio model choices on the bacterial classification sensitivity and specificity can be found elsewhere.⁵ Measured spectral lines were normalized to the sum of the integrated intensity of all measured lines to account for any variation in intensity due to the amount of material ablated.

Sterilization was performed by autoclaving the 1.5 mL bacterial suspension for 40 min prior to deposition on the filter. The deposition was then performed in the same manner as the live samples as described above. Some of the suspension was then used to re-streak a TSA plate and incubated for 2 days to confirm sterilization. No regrowth was observed from the autoclaved specimens.

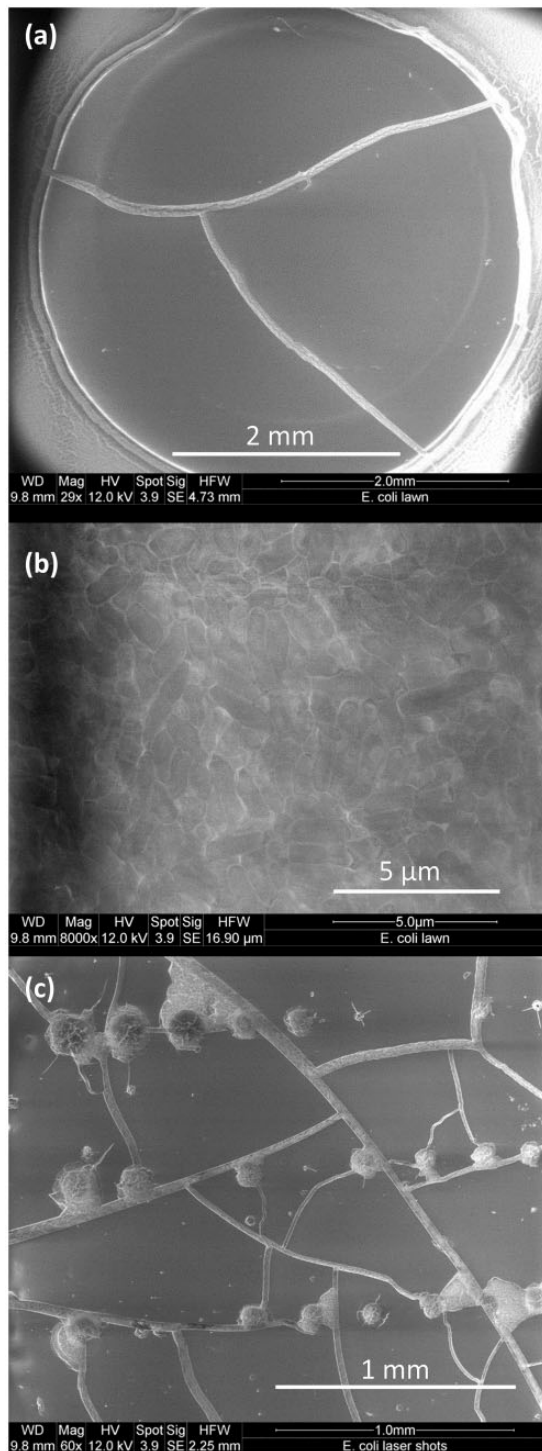


Figure 4. SEM images of bacteria after deposition on the filter paper. (a) One of the three bacterial pads on the filter. After drying, the bacteria formed a smooth, glasslike surface. Cracks formed as the drying occurred. (b) The bacteria were deposited with uniform coverage with no gaps or visible height variations. Individual cells are clearly visible. (c) Laser shots resulted in a fracturing of the glassy surface of the bacterial pad, with multiple cracks and other damage being evident. Craters varied in size, averaging approximately 100 μm .

Results

Classification

For each of the four species, approximately 350–400 spectra were acquired over the course of approximately three months and analyzed using both discriminant function analysis (DFA) and partial least squares discriminant analysis (PLS-DA), both of which have been discussed previously.⁵ These spectra were acquired from multiple filters and multiple generations of bacteria (from multiple growth plates and multiple suspensions) to ensure that any variation observed in the analysis was representative of changes in the bacteria itself and not any small differences in preparation. This provided a large, robust library for discrimination. A truly robust library attempts to account for all possible sources of variation that may be encountered in future unknown specimens by itself containing a large number of data points per classification group acquired under as many conditions as possible and excluding no outliers encountered during construction of the library.

The quality of the library and the classification was assessed using an “external validation” in which all the spectra acquired from a single prepared filter were withheld from the library then classified using the remaining spectra acquired from different filters on different days. This was done to eliminate bias in the classification toward data that was acquired at the same time. The results of the DFA on this new library are given in Figure 5 which shows a classification library composed of 1513 individual spectra from four bacterial species. Confusion matrices or truth tables for the external validation tests of this library by both DFA and PLS-DA are given in Table 1.

The quality of a classification test is best described by the test’s sensitivity, or true positive rate, and specificity, the true negative rate. Using DFA, the library possessed a sensitivity of $98 \pm 2\%$ and a specificity of $99 \pm 1\%$. Using PLS-DA, the library possessed a sensitivity of $97 \pm 3\%$ and a specificity of $99 \pm 2\%$. This performance was identical within uncertainty. For comparison, testing of bacterial spectra acquired on an agar medium utilizing RM2 gave a sensitivity and specificity, respectively, of $91 \pm 16\%$ and $97 \pm 9\%$ for DFA and $93 \pm 10\%$ and $91 \pm 21\%$ for PLS-DA.⁵

Concentration

Serial dilutions of the standard *E. coli* suspension were made corresponding to fractional concentrations of $c = 1, 0.1, 0.075, 0.066, 0.05, 0.033, 0.025, 0.0125, \text{ and } 0.01$. After deposition, these suspensions provided from 10^6 ($c = 1$) to 10^4 ($c = 0.01$) cells per ablation event. For this study, *E. coli* was used as the representative bacterial species, as no significant dependence on the species of bacteria was anticipated. Seventeen single-shot spectra were acquired at each concentration. For each spectrum the sum of the integrated area under all of the peaks used for classification

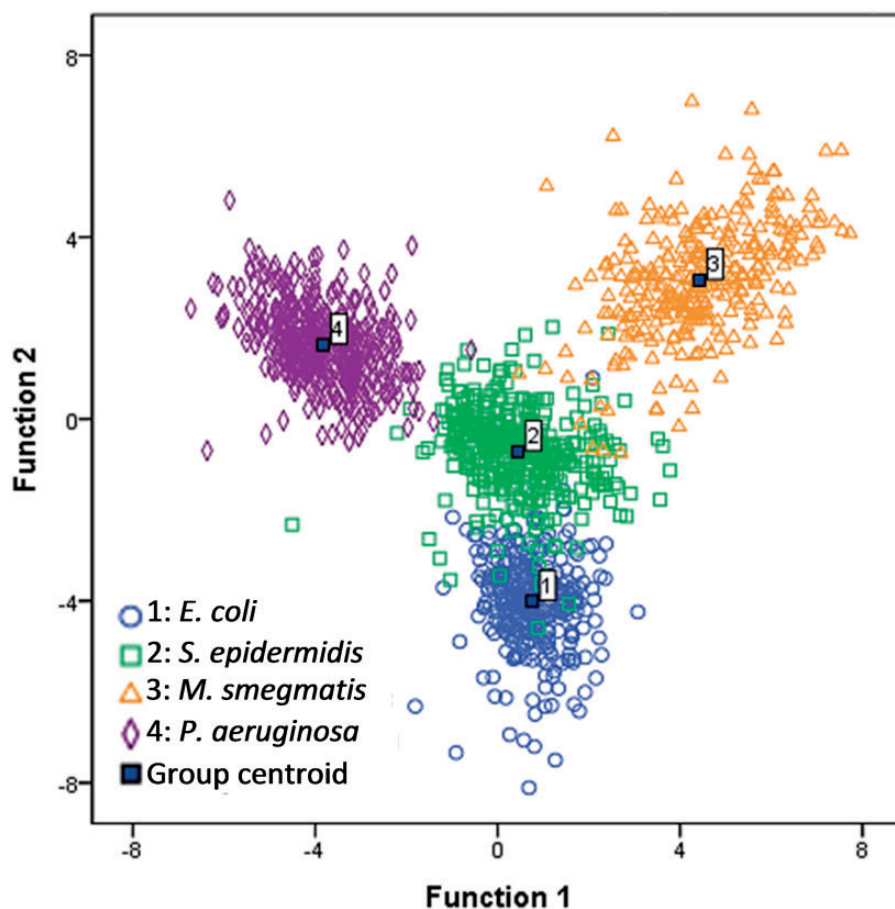


Figure 5. The first two discriminant function scores of a DFA performed on 1513 spectra acquired from live bacteria deposited on nitrocellulose filters. Each spectrum was down-selected to 164 independent variables utilizing a combination of emission peak intensities and ratios (RM3) prior to analysis.

Table 1. Truth table results for two multivariate techniques (DFA and PLS-DA) utilized in an externally-validated classification of four bacterial genera.

DFA			PLS-DA		
	True	False		True	False
<i>Escherichia</i>			<i>Escherichia</i>		
Positive	98.28%	0.77%	Positive	96.55%	1.12%
Negative	99.23%	1.72%	Negative	98.88%	3.45%
<i>Staphylococcus</i>			<i>Staphylococcus</i>		
Positive	97.75%	1.44%	Positive	96.75%	1.53%
Negative	98.56%	2.25%	Negative	98.47%	3.25%
<i>Pseudomonas</i>			<i>Pseudomonas</i>		
Positive	99.57%	0.22%	Positive	98.92%	0.33%
Negative	99.78%	0.43%	Negative	99.67%	1.08%
<i>Mycobacterium</i>			<i>Mycobacterium</i>		
Positive	95.36%	0.33%	Positive	97.02%	0.41%
Negative	99.67%	4.64%	Negative	99.59%	2.98%
Sensitivity	98 ± 2%		Sensitivity	97 ± 3%	
Specificity	99 ± 1%		Specificity	99 ± 2%	

was calculated. This sum is denoted as the “total emission intensity.” The average total emission intensity for the 17 spectra as a function of cell concentration is shown in Figure 6. The associated uncertainty bars are the one-sigma standard deviations of the 17 measurements. In the typical low-concentration regime of a LIBS calibration curve, the measured LIBS intensity is linearly dependent on the concentration of the analyte up to a saturation point, where the intensity can become relatively constant. The bacterial serial dilutions behaved in a similar fashion (as can be seen in the Figure 6 inset) with a saturation or flattening out of the LIBS total emission intensity observed at concentrations greater than $c = 0.1$ corresponding to 10^5 cells per shot or more. This total emission intensity decreased in a linear fashion to a minimum noise value at approximately $c = 0.01$. Because the total emission intensity included the observed emission from the carbon 247 nm line which was the dominant feature of the blank nitrocellulose filter spectrum (Figure 3a), this value never went to zero in the absence of any bacterial cells.

This behavior matched the expected trend, although the variations in measurements were very high at lower concentrations. It is believed that this was caused by bacteria clumping together, forming some areas of high concentration and some areas of bare filter, rather than a thinner but still smooth bacterial pad as was observed at the full concentration (essentially one large and continuous clump). Attempts are currently being made to allow for more uniform distribution at any concentration.

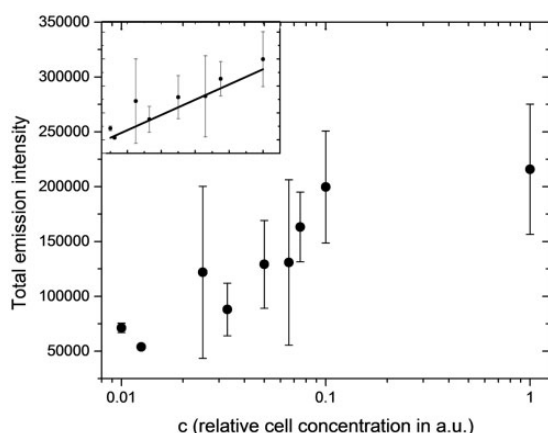


Figure 6. A log-lin calibration curve for bacterial samples. A concentration of $c = 1$ corresponded to 10^{11} cells/mL as determined by optical densitometry resulting in approximately 10^6 cells per ablation. This was the concentration achieved by transferring 24 h of growth for *E. coli* from a TSA plate to 1.5 mL distilled water. The inset shows a linear fit to the lowest eight concentrations on a lin-lin plot.

Sterilization

Autoclaved *E. coli* was prepared and data were taken in the same method as described previously. LIBS spectra were then compared to the live bacterial library using a discriminant function analysis. Because DFA cannot produce a null result, meaning that an unidentified sample must be classified as one of the classes in the library, all spectra from autoclaved sterilized *E. coli* classified consistently (100%) as live *E. coli* even though the plot of the first two discriminant function scores clearly indicates a detectable and reproducible difference between live and dead cells (Figure. 7). It has been proposed previously that this effect is due to autoclave-induced cell lysis and the subsequent omission of nuclear material or other cellular material from the LIBS spectrum.¹⁶ If this is indeed the case, the new methodology described here would allow for this effect to be more readily observed as cellular contents lost in lysis would presumably be lost through the filter paper that might otherwise be retained on an agar plate. These results are currently under investigation using other destructive and nondestructive inactivation techniques such as sonication and UV inactivation, respectively.

Conclusions

The introduction of a new mounting technique resulted in a LIBS-based bacterial discrimination that more closely resembled the techniques with which pathologists and clinicians are already comfortable and is more realistic in a clinical setting. This method also allowed for faster sample preparation and removed the necessity for centrifugation from the process. While the introduction of nitrocellulose filters introduced a carbon background signal to the bacterial spectrum, this did not result in any reduction in the accuracy of the technique for discrimination. In fact, the accuracy of the technique as determined by the calculated sensitivity and specificity of a four genus live bacteria test was improved since this method was implemented.

This introduction of a new mounting protocol has currently increased the required number of cells for measurements to be taken. This is due to the intensity of the carbon 247 nm line from the filter which limits the amplification of the camera which can be used, and it also seems to be related to a clumping of the bacterial cells upon deposition. Should a more uniform lawn of low concentration cells be achieved, this problem can be overcome.

A DFA of autoclaved cells tested against a library of live cells showed a spectral difference between live and dead *E. coli* that was previously unobserved by our group but that has been indicated recently by other groups. This is currently believed to be a result of material lost through the filter paper after the lysis of cells. This new mounting method allows for this possibility to be investigated more thoroughly in future experiments.

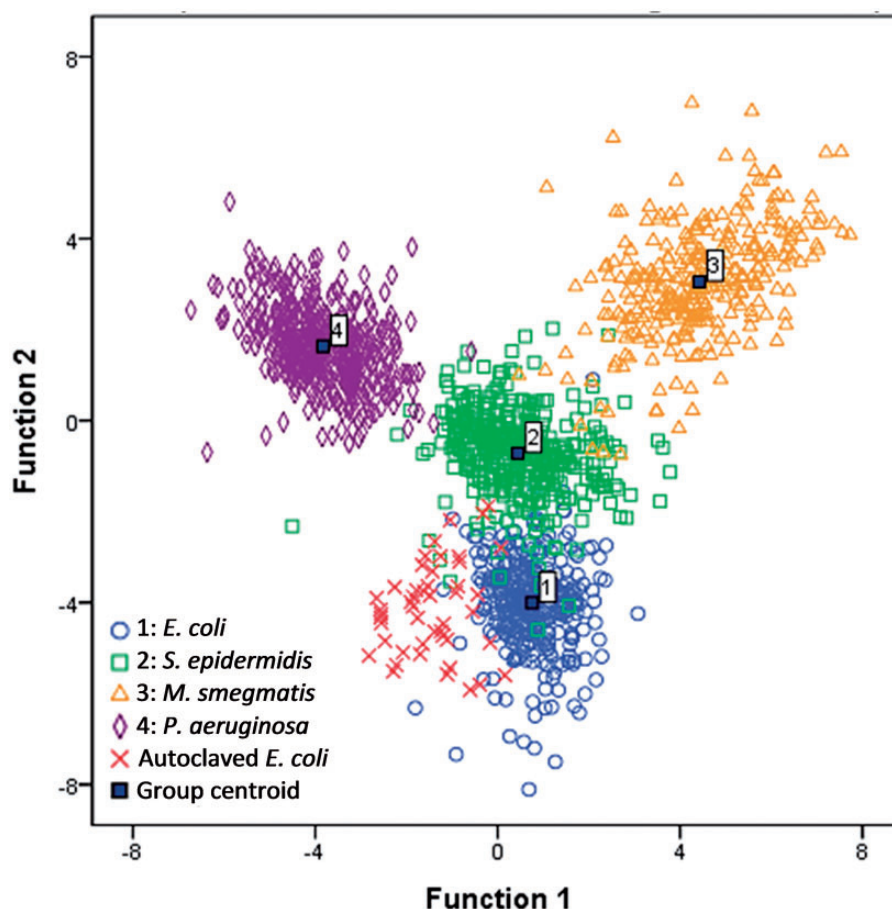


Figure 7. Discriminant function one and two scores from an external test of unclassified *E. coli* samples sterilized via autoclaving (“x”) against the library of live bacteria. While these data most closely resembled live *E. coli* (open circles), classifying as 100% *E. coli*, they possessed a distinctly different discriminant function one score as evidenced by the systematic shift to lower scores away from the centroid of group 1.

Acknowledgments

The authors thank Ms Ingrid Churchill and Dr Andrew Hubberstey for their continual support of the bacterial preparation aspects of this project.

Conflict of Interest

The authors report there are no conflicts of interest.

Funding

The authors received financial support of an NSERC Discovery and RTI equipment grant as well as a Canada Foundation for Innovation–Ontario Innovation Fund infrastructure grant. DJG was supported in part by the University of Windsor’s Outstanding Scholars program.

References

1. A.C. Samuels, F.C. DeLucia Jr., K.L. McNesby, A.W. Miziolek. “Laser-Induced Breakdown Spectroscopy of Bacterial Spores, Molds, Pollens, and Protein: Initial Studies of Discrimination Potential”. *Appl. Opt.* 2003. 42(30): 6205–6209.
2. S. Morel, M. Leone, P. Adam, J. Amouroux. “Detection of Bacteria by Time-Resolved Laser-Induced Breakdown Spectroscopy”. *Appl. Opt.* 2003. 42(30): 6184–6191.
3. J.D. Hybl, G.A. Lithgow, S.G. Buckley. “Laser-Induced Breakdown Spectroscopy Detection and Classification of Biological Aerosols”. *Appl. Spectrosc.* 2003. 57(10): 1207–1215.
4. S. Manzoor, S. Moncayo, F. Navarro-Villoslada, J.A. Ayala, R. Izquierdo-Hornillos, F.J. Manuel deVillena, J.O. Caceres. “Rapid Identification and Discrimination of Bacterial Strains by Laser-Induced Breakdown Spectroscopy and Neural Networks”. *Talanta*. 2014. 121: 65–70.
5. R.A. Putnam, Q.I. Mohaidat, A. Daabous, S.J. Rehse. “A Comparison of Multivariate Analysis Techniques and Variable Selection Strategies in a Laser-Induced Breakdown Spectroscopy Bacterial Classification”. *Spectrochim. Acta, Part B*. 2013. 87: 161–167.
6. S.J. Rehse, H. Salimnia, A.W. Miziolek. “Laser-Induced Breakdown Spectroscopy (LIBS) An Overview of Recent Progress and Future Potential for Biomedical Applications”. *J. Med. Eng. Technol.* 2012. 36(2): 77–89.
7. R. Multari, D.A. Cremers, J.M. Dupre, J.E. Gustafson. “The Use of Laser-Induced Breakdown Spectroscopy for Distinguishing

- Between Bacterial Pathogen Species and Strains". *Appl. Spectrosc.* 2010. 64(7): 750–759.
8. R.A. Multari, D.A. Cremers, J.M. Dupre, J.E. Gustafson. "Detection of Biological Contaminants on Foods and Food Surfaces Using Laser-Induced Breakdown Spectroscopy (LIBS)". *J. Agric. Food Chem.* 2013. 61: 8687–8694.
 9. J.L. Gottfried. "Discrimination of Biological and Chemical Threat Simulants in Residue Mixtures on Multiple Substrates". *Anal. Bioanal. Chem.* 2011. 400: 3289–3301.
 10. S.J. Rehse, N. Jeyasingham, J. Diedrich, S. Palchadhuri. "A Membrane Basis for Bacterial Identification and Discrimination Using Laser-Induced Breakdown Spectroscopy". *J. Appl. Phys.* 2009. 105(10): 102034–102034.
 11. S.J. Rehse, J. Diedrich, S. Palchadhuri. "Identification and Discrimination of *Pseudomonas aeruginosa* Bacteria Grown in Blood and Bile by Laser-Induced Breakdown Spectroscopy". *Spectrochim. Acta, Part B.* 2007. 62: 1169–1176.
 12. R.A. Multari, D.A. Cremers, M.L. Bostian, J.M. Dupre, J.E. Gustafson. "Proof of Principle for a Real-Time Pathogen Isolation Media Diagnostic The Use of Laser-Induced Breakdown Spectroscopy to Discriminate Bacterial Pathogens and Antimicrobial-Resistant *Staphylococcus aureus* Strains Grown on Blood Agar". *J. Pathogens.* 2013. 2013: 898106–898106.
 13. Q.I. Mohaidat, K. Sheikh, S. Palchadhuri, S.J. Rehse. "Pathogen Identification With Laser-Induced Breakdown Spectroscopy The Effect of Bacterial and Biofluid Specimen Contamination". *Appl. Opt.* 2012. 51(7): B99–B107.
 14. C. Barnett, C. Bell, K. Vig, C.A. Akpovo, L. Johnson, S. Pillai, S. Singh. "Development of a LIBS Assay for the Detection of *Salmonella enterica* serovar Typhimurium from Food". *Anal. Bioanal. Chem.* 2011. 400: 3323–3330.
 15. S.J. Rehse, Q.I. Mohaidat, S. Palchadhuri. "Towards the Clinical Application of Laser-Induced Breakdown Spectroscopy for Rapid Pathogen Diagnosis the Effect of Mixed Cultures and Sample Dilution on Bacterial Identification". *Appl. Opt.* 2010. 49(13): C27–C35.
 16. P. Sivakumar, A. Fernandez-Bravo, L. Taleh, J.F. Biddle, N. Melikechi. "Detection and Classification of Live and Dead *Escherichia coli* by Laser-Induced Breakdown Spectroscopy". *Astrobiol.* 2015. 15(2): 144–153.
 17. Q. Mohaidat, S. Palchadhuri, S.J. Rehse. "The Effect of Bacterial Environmental and Metabolic Stresses on a LIBS-Based Identification of *Escherichia coli* and *Streptococcus viridans*". *Appl. Spectrosc.* 2011. 65(4): 386–392.
 18. J. Diedrich, S.J. Rehse, S. Palchadhuri. "Escherichia coli Identification and Strain Discrimination Using Nanosecond Laser-Induced Breakdown Spectroscopy". *Appl. Phys. Lett.* 2007. 90(16): 163901–163901.
 19. D.E. Lewis, J. Martinez, C.A. Akpovo, L. Johnson, A. Chauhan, M.D. Edington. "Discrimination of bacteria from Jamaican Bauxite Soils Using Laser-Induced Breakdown Spectroscopy". *Anal. Bioanal. Chem.* 2011. 401: 2225–2236.
 20. V.N. Rai, A.K. Rai, F.-Y. Yueh, J.P. Singh. "Optical Emission from Laser-Induced Breakdown Plasma of Solid and Liquid Samples in the Presence of a Magnetic Field". *Appl. Opt.* 2003. 42(12): 2085–2093.